Biogeosciences Discuss., 9, 4099–4132, 2012
www.biogeosciences-discuss.net/9/4099/2012/
doi:10.5194/bgd-9-4099-2012

Biogeosciences Discussions

High temporal and spatial variability of dissolved oxygen and pH in a nearshore California kelp forest

C. A. Frieder[1], S. H. Nam[2], T. R. Martz[3], and L. A. Levin[1,4]

[1]Integrative Oceanography Division, Scripps Institution of Oceanography, University of California San Diego, 9500 Gilman Drive, La Jolla, CA 92093-0218, USA
[2]Climate, Atmospheric Science and Physical Oceanography, Scripps Institution of Oceanography, University of California San Diego, 9500 Gilman Drive, La Jolla, CA 92093-0230, USA
[3]Geosciences Research Division, Scripps Institution of Oceanography, University of California San Diego, 9500 Gilman Drive, La Jolla, CA 92093-0244, USA
[4]Center for Marine Biodiversity and Conservation, Scripps Institution of Oceanography, University of California San Diego, 9500 Gilman Drive, La Jolla, CA 92093-0218, USA

Received: 13 March 2012 – Accepted: 16 March 2012 – Published: 30 March 2012

Correspondence to: C. A. Frieder (ctanner@ucsd.edu)

Published by Copernicus Publications on behalf of the European Geosciences Union.

Abstract

Predicting consequences of ocean deoxygenation and ocean acidification for nearshore marine ecosystems requires baseline dissolved oxygen (DO) and carbonate chemistry data that are both high-frequency and high-quality. Such data allow accurate assessment of environmental variability and present-day organism exposure regimes. In this study, scales of DO and pH variability were characterized over one year in a nearshore, kelp forest ecosystem in the Southern California Bight. DO and pH were strongly, positively correlated revealing that organisms on this upwelling shelf are not only exposed to low pH but also low DO. The dominant temporal scale of DO and pH variability occurred on semidiurnal, diurnal and event (days–weeks) time scales. Daily ranges in DO and pH at 7 m water depth (13 mab) could be as large as 220 μmol kg^{-1} and 0.36 units, respectively. This range is much greater than the expected decreases in pH in the open ocean by the year 2100. Sources of pH and DO variation include photosynthesis within the kelp forest ecosystem, which can elevate DO and pH by up to 60 μmol kg^{-1} and 0.1 units over one week following the intrusion of high-density, nutrient-rich water. Accordingly, highly productive macrophyte-based ecosystems could serve as deoxygenation and acidification refugia by acting to elevate DO and pH relative to surrounding waters. DO and pH exhibited greater spatial variation over a 10 m increase in water depth (from 7 to 17 m) than along a 5-km stretch of shelf in a cross-shore or alongshore direction. Over a three-month time period mean DO and pH at 17-m water depth were 168 μmol kg^{-1} and 7.87, respectively. These values represent a 35 % decrease in mean DO and 37 % increase in [H$^+$] relative to surface waters. High-frequency variation was also reduced at depth. The mean daily range in DO and pH was 39 % and 37 % less, respectively, at 17-m water depth relative to the surface. As a consequence, the exposure history of an organism is largely a function of its depth of occurrence within the kelp forest. These findings raise the possibility that the benthic communities along eastern boundary current systems are currently acclimatized and adapted to natural, variable, and low DO and pH. Future exposure of

Title Page

Abstract | Introduction

Conclusions | References

Tables | Figures

Back | Close

Full Screen / Esc

Printer-friendly Version

Interactive Discussion

coastal California populations to low DO and pH may increase as upwelling intensifies and hypoxic boundaries shoal, compressing habitats and challenging the physiological capacity of intolerant species.

1 Introduction

Increased levels of atmospheric carbon dioxide (CO_2) have reduced subsurface oxygen concentrations and increased acidity of surface waters (Gruber, 2011; Doney et al., 2012). Ocean deoxygenation is due to a combination of warming, increased stratification and altered ocean circulation (Keeling et al., 2010). Ocean acidification is an increase in oceanic CO_2 uptake and the concomitant decrease in seawater pH (Doney et al., 2009). Much of what has been learned about pH and DO trends and trajectories in the ocean is based upon open-ocean conditions measured via ship-based hydrographic time series that sample quarterly, annually or even less often. This limits our understanding of DO and pH dynamics in nearshore settings to annual frequencies and lower.

The coastal environment is a highly variable system. Fluctuations in temperature, salinity, air-sea gas exchange, mixing processes and biogeochemical processes can have large influences on DO and pH. There are contemporary nearshore environments, particularly eastern boundary current systems, which are exposed to low pH conditions during upwelling events (Feely et al., 2008; Hofmann et al., 2011b). Deoxygenation and acidification are of particular concern in tandem in ocean regions where DO and pH are tightly linked through local primary production and/or remineralization of organic matter (Gruber, 2011; Hofmann et al., 2011a). Understanding the nature and drivers of DO and pH dynamics along eastern boundary current systems, which harbor ecologically and economically important species, will provide insight into the relative sensitivity of these systems to a changing ocean climate.

There has been much emphasis on understanding the physical characteristics of nearshore waters in upwelling systems, and different scales of variability have been

BGD
9, 4099–4132, 2012

identified and associated with specific processes. Sources of variability in temperature and nutrients, for example, include El Niño–Southern Oscillation (ENSO), seasonal and temporal upwelling, coastally trapped waves, coastal sea breeze, and internal tidal waves and bores (Lluch-Cota et al., 2001; Pringle and Riser, 2003; Kaplan et al., 2003; Lerczak et al., 2001; Pineda, 1999), but there is presently limited information regarding DO and pH dynamics in relation to these different scales of variability. Recent studies have found that the upper horizon of the hypoxic boundary (defined as 60 µmol kg^{-1}) in the Southern California Bight (SCB) has shoaled by almost 100 m near the coastline since the 1980's (Bograd et al., 2008), with consequences for benthic fishes (McClatchie et al., 2010). ENSO cycles also influence DO over the SCB shelf. The 2010 La Niña event led to a 38–50 % decline in DO relative to the normal seasonal mean (Nam et al., 2011). Strong upwelling events also bring low pH water toward the surface along the Eastern Pacific margin with pH values falling below 7.7 near the coastline (Feely et al., 2008). Knowledge of pH and DO dynamics on shorter time scales is even more limited, and is the focus of this study.

The SCB is characterized by water masses from the subarctic and tropical Pacific through the California Current and California Undercurrent (Bray et al., 1999; Dong et al., 2009). Seasonal upwelling is strongest during the spring when equatorward currents lift isopycnal surfaces and bring low DO and low pH water from intermediate depths onto the continental shelf (Bray et al., 1999; Feely et al., 2008). The complex bathymetry and coastline of the SCB drives extensive variability in circulation features, and coastal regions are affected by both local and coastally propagating remote forcing which drives temporal upwelling events at timescales of a few days to weeks (Pringle and Riser, 2003; Dong et al., 2009; Nam and Send, 2011). The SCB also harbors one of the world's fastest growing primary producers, the giant kelp *Macrocystis pyrifera*. Kelp forests are abundant along the SCB coast (North et al., 1993), and serve as the foundation for diverse and energy-rich habitats of great ecological and economic importance (Graham et al., 2007). Understanding the DO and pH dynamics within kelp

BGD
9, 4099–4132, 2012

forests will provide detailed information regarding the corresponding exposure histories for a diversity of valued species of molluscs, echinoderms, crustaceans and fishes.

Here we characterize nearshore DO and pH conditions in the La Jolla Kelp Forest (LJKF). We deployed two sensors in a variety of configurations in order to ask the following questions: What are the dominant short-term scales of pH and DO variability? Is there spatial variation in pH and DO within the kelp forest linked to depth, alongshore direction, or cross-shore direction? What is the relationship between pH and DO in the kelp forest and is the relationship stable in time and space? To place these results in a biological context we consider how spatial and temporal heterogeneity in pH and DO may influence different levels of biological organization and organism exposure histories.

2 Methods

2.1 Field measurements

We used moorings deployed on the inner shelf, located within and around the LJKF to explore cross-shore, alongshore and water depth effects on DO and pH between July 2010 and November 2011 (Fig. 1). The shelf in this region is 8 km wide and the kelp forest, at its fullest extent, is 8 km long and up to ~ 1.5 km wide. Time-series data were collected with a sampling rate of 15 min using two instruments placed in different configurations among moorings (Fig. 1). Data were nearly continuously collected from mooring A (32.81° N 117.29° W; 20 m bottom depth) within the LJKF. The sensor was attached 13 meters above bottom (mab or 7 m water depth) to explore variability in DO and pH over multiple temporal scales (Fig. 1a). Changes in DO and pH with water depth were investigated by comparing concurrent data from mooring A at 7 m and 17 m (3 mab) below the surface (Fig. 1b). These depths are hereafter referred to as "shallow water" and "deep water". Alongshore changes in DO and pH were explored by comparing sensor data from 7 m water depth from mooring A and mooring D (32.85° N

BGD
9, 4099–4132, 2012

117.28° W; 20 m bottom depth), which was located 5 km to the north in an alongshore direction and still within the LJKF (Fig. 1c). Cross-shore changes in DO and pH were explored by comparing sensor data from 7 m water depth at different locations along an east-west transect perpendicular to the local coastline (Fig. 1d). In 2010, the paired moorings were mooring B, 3.5 km from the coast (32.81° N 117.31° W; 30 m bottom depth), and mooring A, 1.9 km from the coast. Mooring B is located offshore of the kelp forest. In 2011, the paired moorings were mooring A (1.9 km) and mooring C, 1.4 km from the coast (32.81° N 117.28° W; 15 m bottom depth). Concurrent DO and pH data exist for all deployments except that no pH data were available from August to November 2011 at mooring A due to a sensor malfunction.

Data were collected using two "SeapHOx" instrument packages. The SeapHOx consists of a Honeywell Durafet III pH sensor (Martz et al., 2010), an Aanderaa 3835 oxygen optode, and an SBE-37 MicroCAT CTD. One of the MicroCAT CTDs was equipped with a pressure sensor. We compared LJKF data with current speed and direction measured in the upper 30 m of the water column (100 m bottom depth) from a nearby mooring located 14 km to the NW (DM Buoy: 32.94° N 117.32° W). Current data were obtained every 7.5 min at 5 m intervals from 5 to 100 m using a down-looking 300 kHz acoustic Doppler current profiler (ADCP).

2.2 Calibrations

To calibrate the pH sensors, discrete water samples were taken during each SeapHOx deployment for the determination of total alkalinity (TA) and total dissolved inorganic carbon (DIC) (Fig. 1a). The calibration samples were collected via SCUBA next to the sensor with a 5 l niskin bottle. The collected seawater was transferred to a 500 ml clean borosilicate glass bottle with a ground glass neck and stopper. The samples were poisoned with a saturated mercuric chloride solution. TA measurements were determined using an open-cell, potentiometric titration (Dickson et al., 2007). DIC measurements were determined by acid extraction and coulometric detection of CO_2 (Dickson et al., 2007). pH was calculated from TA and DIC using the Matlab version of CO2SYS (van

BGD
9, 4099–4132, 2012

Heuven et al., 2011) as recommended by Dickson et al. (2007). The calculated pH at in situ temperature from the calibration sample was used to determine the electrode-specific calibration coefficients. The calibration sample produced a pH accuracy of 0.01 units for each SeapHOx instrument. The oxygen sensors were factory calibrated by Aanderaa and before each deployment a two-point (0 % and 100 % saturation) offset was applied as recommended in the manual.

2.3 Data analysis

DO and pH data from the SeapHOx sensors were analyzed as either un-filtered data in order to illustrate the extremes and rates of change or a 2-d running mean was applied to raw data. pH is reported on the total hydrogen ion scale at in situ temperature. Extreme salinity outliers (≥ 3 SD) were removed, and density was calculated from salinity and temperature data. Time in all figures is shown in Coordinated Universal Time (UTC). Although uptake and release of dissolved inorganic carbon leads to a slightly non-linear relationship between pH and DO, for the purposes of our statistical description a simple linear fit between the two was sufficient to distinguish underlying patterns and the use of higher order functions was deemed unnecessary. Accordingly, the relationship between DO and pH was determined with a Model-II least squares fit for all concurrent data of DO and pH. Spectral analyses were calculated on detrended datasets using a fast fourier transform. Spectra of temperature, DO and pH were averaged over four, 16-d windows from the longest continuous deployment at mooring A 7 m below the surface from 25 January 2011–31 March 2011. Pressure data were not available during this time period. Instead spectra were averaged over four, 11.5-d windows from 29 July 2010–13 September 2010 and averaging yields a typical power spectrum of pressure for this region. To explore DO, pH, and temperature cycles at semidiurnal and diurnal timescales, a fast fourier transform was applied to data and desired frequencies were bandpass filtered (e.g. $DO_{f=1}$). Current data obtained from the DM mooring were decomposed into cross-shore (u) and alongshore (v) components and both were smoothed with a 2-d running mean. Equatorward phases were

BGD
9, 4099–4132, 2012

designated as time periods when alongshore current at all depths between 5 and 30 m was southward, e.g. $v < 0$, and poleward phases were designated as time periods when alongshore current velocity at all depths between 5 and 30 m was northward, e.g. $v > 0$.

3 Results

3.1 Temporal variability in dissolved oxygen and pH

3.1.1 Diurnal and semidiurnal scales of dissolved oxygen and pH variability

Two time scales of periodic variability were identified within one year at mooring A: semidiurnal and diurnal. The average daily range (peak-to-peak) in DO and pH were 63 µmol O_2 kg^{-1} (n = 249 d; SD = 39.4) and 0.11 pH units (n = 169 d; SD = 0.07). The daily range could be as great as 220 µmol O_2 kg^{-1} and 0.36 pH units. DO, pH, temperature and pressure at 7 m water depth exhibited energetic variance at both the semidiurnal and diurnal frequencies (Fig. 2). Semidiurnal variance was greater than diurnal variance for temperature and pressure, but diurnal variance was greater than semidiurnal variance for DO and pH. Semidiurnal and diurnal DO and pH fluctuations had differing proportions of physical and biological forcing. Semidiurnal fluctuations in DO and pH were well correlated with temperature, suggesting that the primary source of semidiurnal variability was physical isothermal fluctuations ($\mathrm{DO}_{f=2} = 20.8 * \mathrm{temp}_{f=2}$, $R^2 = 0.85$; $\mathrm{pH}_{f=2} = 0.03 * \mathrm{temp}_{f=2}$, $R^2 = 0.74$). DO and pH were less correlated with temperature at the diurnal band ($\mathrm{DO}_{f=1} = 22.1\mathrm{temp}_{f=1}$, $R^2 = 0.55$; $\mathrm{pH}_{f=1} = 0.04 * \mathrm{temp}_{f=1}$, $R^2 = 0.53$). A decrease in correlation at the diurnal bandwidth indicates that diurnal isothermal fluctuations either play less of a role in diurnal forcing of DO and pH or other mechanisms (e.g., diel scales of production and respiration, and/or air-sea gas exchange associated with diurnal land-sea breeze) are opposing diurnal modulations in DO and pH forced by temperature. These identified high-frequency scales

BGD
9, 4099–4132, 2012

of fluctuations in the LJKF are not only persistent through time but also encompass a large range of DO and pH conditions.

3.1.2 Event-scale variability in dissolved oxygen and pH

Overall increases and decreases in DO and pH, and intermittent amplifications of higher frequency (e.g., diurnal and semidiurnal) fluctuations lasting from days to weeks, were observed in the LJKF. Here we define changes in pH and DO lasting > one day to multiple weeks as event-scale variability.

Mean increases in DO and pH. Notable increases in DO and pH were observed for approximately a week following the occasional intrusion of high-density (deep, cold, and nutrient-rich) water. High-density waters were defined as $\sigma > 25.1\,\mathrm{kg\,m^{-3}}$. This value has been suggested to reflect water containing the threshold concentration of nitrate required for kelp growth (Parnell et al., 2010). During 2010–2011 there were seven events among all moorings when high-density seawater shoaled to 7 m water depth (Table 1). These events fueled primary production and increased DO and pH with the exception of the August 2010 event at mooring B, when high mean DO (290 $\mu\mathrm{mol\,kg^{-1}}$) existed prior to the intrusion of high-density seawater. ΔDO and ΔpH were calculated as the difference between the mean value for seven days before the intrusion of high-density seawater and the mean value for seven days after the intrusion of high-density seawater. The magnitude of the regional water velocity after the event (e.g., v after) explained 62 % of the variation in ΔpH ($\Delta\mathrm{pH} = 0.012 * v$ after $-$ 0.02, $R^2 = 0.62$, $P = 0.035$). The greatest ΔDO and ΔpH values occurred when alongshore currents transitioned from equatorward to strong poleward currents. As an illustrative example, such an event occurred during late April–early May 2011 at mooring D (Fig. 3). Mean DO at $\sigma < 25.1$ prior to the event was 247 $\mu\mathrm{mol\,kg^{-1}}$, and mean DO at $\sigma < 25.1$ the subsequent week was 309 $\mu\mathrm{mol\,kg^{-1}}$, equating to a 20 % increase in DO. The corresponding mean pH before and after the event was 8.07 and 8.17, respectively. Similar observations were made during the same time period in south LJKF (mooring A). Mean DO before the event was 249 $\mu\mathrm{mol\,kg^{-1}}$, and mean DO after the

BGD
9, 4099–4132, 2012

event was 312 µmol kg^{-1}. The corresponding mean pH before and after the event at mooring A was 8.05 and 8.15, respectively. The influx of high-density, nutrient-replete water masses occurred when alongshore current direction was equatorward and was followed by a strong poleward reversal that allowed biological production within the LJKF to release DO, uptake CO_2, and thus increase pH.

Mean decreases in DO and pH. Event-scale mean decreases in DO and pH were rare at 7 m water depth but were observed during Fall 2010 and 2011 (Table 2). In 2010, mean DO and pH dropped below 200 µmol kg^{-1} and 7.9 units for an extended period of time on two occasions. The first event lasted for two days from 4–5 September 2010, and the end of the second event was not captured but lasted > 1.4 d. In 2011, mean DO dropped below 200 µmol kg^{-1} four times (corresponding pH data not available). Each event lasted between one and five days.

Changes in DO and pH variability regimes. We have documented large daily ranges in pH and DO, with magnitudes corresponding to alongshore current direction. Daily DO and pH ranges were greatly enhanced when alongshore currents were equatorward (Fig. 4). As an example, between 29 September 2010–9 November 2010, DO and pH varied up to 113 µmol kg^{-1} d^{-1} and 0.22 units d^{-1}, respectively. When alongshore currents were directed poleward, the maximum daily range in DO and pH was reduced to 40 µmol kg^{-1} and 0.01 units, respectively.

3.2 Spatial variability in dissolved oxygen and pH

3.2.1 Changes in dissolved oxygen and pH with water depth

Simultaneous measurements at 7 and 17 m documented large differences in mean DO and pH over small depth scales within the kelp forest (Fig. 5). Mean DO and pH in shallow water were 259 µmol kg^{-1} and 8.07, respectively. Only 10 m deeper, mean DO and pH were 168 µmol kg^{-1} and 7.87. These represent a 35 % decrease and 37 % increase in DO and [H^+], respectively, from 7 to 17 m. Deep DO and pH were below 130 µmol kg^{-1} and 7.8 for 20 % of the time, and the minimum DO and pH observed

BGD
9, 4099–4132, 2012

were 86 µmol kg^{-1} and 7.67, respectively. Over this 10-m depth range, the average DO and pH gradients were 9 µmol kg^{-1} m^{-1} and 0.02 pH units m^{-1}. The large differences between the DO and pH environment were related to the strength of density stratification (Fig. 6a,b). When the water column was well-stratified DO and pH decreased with increasing depth. A density difference of 0.2–1 kg m^{-3} could equate to a 0.4 unit decrease in pH and a DO reduction of 170 µmol kg^{-1}. On one occasion, starting on 19 December 2010, the water column was well-mixed, but on the fourth day DO and pH steadily decreased at 17 m while remaining stable near the surface; there was no apparent stratification between depths ($\sigma_{7\,\mathrm{m}} \approx \sigma_{17\,\mathrm{m}}$, Fig. 5). This suggests that the P:R relationship in deep water was below one. Variability patterns were also different in deep and shallow water. The mean change per hour in DO in shallow water was 4 µmol kg^{-1} h^{-1} (SD = 7.04), whereas in deep water the mean rate of change was 2.5 µmol kg^{-1} h^{-1} (SD = 4.43). In shallow water the mean change per hour in pH was 0.01 units h^{-1} (SD = 0.02); in deep water the mean rate of change was only 0.006 units h^{-1} (SD = 0.01). Thus, the near-surface DO and pH conditions were more variable on semidiurnal and diurnal timescales, while near-bottom depths (17 m; 3 mab) exhibited more stable high-frequency conditions and large changes were associated with the structure of the water column over event time scales.

3.2.2 Alongshore changes in dissolved oxygen and pH within the kelp forest

Alongshore differences in DO and pH within the kelp forest were examined 5 km apart in an alongshore direction at 7 m water depth. The moorings were located in north and south LJKF. There were minimal but significant differences in DO and pH during the study period (Fig. 7). Mean DO was 258 versus 252 µmol kg^{-1} ($t_{0.05(2),2469} = 5.8$, $P < 0.001$) and mean pH was 8.10 versus 8.05 in north LJKF (mooring D) versus south LJKF (mooring A), respectively ($t_{0.05(2),2469} = 17.5$, $P < 0.001$). The average gradient from north to south in DO and pH were negligible (e.g., < 1.5 µmol kg^{-1} km^{-1} and 0.01 units km^{-1}). Temporal variability was also similar at both sites. Concordant

BGD
9, 4099–4132, 2012

high-frequency, large excursions in DO and pH occurred on diurnal and semidiurnal frequencies at both moorings. Event-scale increases in DO and pH resulting from biological production in response to the intrusion of high-density, high-nutrient seawater were observed in both the north and south LJKF and magnitudes of change were very similar (Table 1; event start = 26 April 2011). This suggests that the spatial scale of these events can span the entire length of the kelp forest (≥ 5 km). However, beginning 16 May 2011 higher density waters, with a low pH and DO signature, were observed in south LJKF but not north LJKF for two days. At that time, the gradient in DO and pH from south to north significantly increased to 20 μmol kg^{-1} km^{-1} and 0.05 units km^{-1}, respectively; mean temperature was 1 °C cooler in south LJKF versus north LJKF. This discrepancy between north and south LJKF was also observed earlier in the month, between 1 May and 6 May 2011. Thus, in general there was a great deal of coherence in DO and pH in north and south LJKF but minor differences existed and were likely related to different local forcing dynamics.

3.2.3 Cross-shore changes in dissolved oxygen and pH on the inner shelf

DO and pH conditions varied strongly with proximity to shore. Mean DO and pH at 7 m decreased with decreasing distance from shore suggesting that isopleths of DO and pH slope up towards the coast (Fig. 8). Two measurement experiments were conducted during the same months (September–November) in 2010 and 2011 along a zonal transect (Fig. 1). During 2010, mean DO was 20 μmol kg^{-1} lower at 1.9 km versus 3.5 km from the coast ($t_{0.05(2),4117} = 37.3$, $P < 0.001$), resulting in a DO gradient of -13 μmol kg^{-1} km^{-1} (towards the coastline). Mean pH was 0.03 units lower ($t_{0.05(2),4117} = 38.5$, $P < 0.001$), and the gradient was -0.02 units km^{-1}. These differences could not be attributed to water mass as the density gradient between moorings was negligible (< 0.01 kg m^{-3} km^{-1}) between the two sites and there was no significant difference in density conditions ($P > 0.05$). The same trend emerged during 2011. Mean DO was 19 μmol kg^{-1} lower at 1.4 km versus 1.9 km from the coast

BGD
9, 4099–4132, 2012

($t_{0.05(2),3064}$ = 15.5, $p < 0.001$), and resulted in a gradient of $-38\,\mu\text{mol kg}^{-1}\,\text{km}^{-1}$. A pH comparison was not available for 2011. Density was greater at the outer mooring ($t_{0.05(2),4117}$ = 3.27, $p < 0.002$). The expectation would be that DO and pH would be greater closer to shore if considering only physical water excursion, but the opposite trend has emerged.

The decoupling between DO and pH with density was investigated by comparing the changes in the linear relationship between DO and pH with density with respect to distance from shore. At a given density, DO and pH were lower inshore relative to offshore, particularly at high-density values. This phenomenon was corroborated by changes in the linear relationship between density and DO or pH with varying distance from shore. There was a significant decrease in the intercept of the linear relationship between density and DO with decreasing distance from shore during both years (2010: $t_{0.05(2),8231}$ = 33.7, $P < 0.001$; 2011: $t_{0.05(2),6125}$ = 14.2, $P < 0.001$). There was also a significant decrease in the intercept of the linear relationship between density and pH with decreasing distance from shore during 2010 ($t_{0.05(2),8231}$ = 14.6, $P < 0.001$). These relationships illustrate the change in the DO and pH environment with proximity to shore was due to shoaling isopleths that were decoupled from isopycnals.

3.3 Relationship between dissolved oxygen and pH

There was a significant, positive linear relationship between DO and pH for all data collected at 7 and 17 m water depths (pH = 0.002 $*$ DO + 7.50, R^2 = 0.96, $P < 0.001$; Fig. 6c). The linear relationship between DO and pH was more stable at depth than near the surface (7 m: R^2 = 0.85, $P < 0.001$; 17 m: R^2 = 0.97, $P < 0.001$). In a cross-shore direction the DO and pH relationship did not vary (Fig. 6d). Between years there was a large offset and change in slope between fall 2010 and fall 2011 (Fig. 6d). The slope was greater in 2011 than in 2010 ($t_{0.05(2),14356}$ = 7.72; $P < 0.001$). The strong relationship between DO and pH indicates a mechanistic link. There were no significant linear relationships between DO or pH and temperature in shallow water

BGD
9, 4099–4132, 2012

(P > 0.05; Fig. 6e,f), but with increasing depth there were positive linear relationships (DO = 32.9 ∗ temp − 2.6, R^2 = 0.62, P < 0.001; pH = 0.08 ∗ temp + 6.88, R^2 = 0.67, P < 0.001). The positive relationship between temperature and DO or pH can be best explained by biologically-driven gradients and is opposite to thermodynamically-predicted changes in temperature with DO or pH. The stronger correlation at depth suggests that physically forced changes via water movement are more important in driving changes in DO and pH in deeper waters, while local biochemical processes and air-sea gas exchange dominate at the surface.

Low DO and pH were linked but high DO and pH were not. The minimum pH and DO values were observed simultaneously at 17 m water depth on 30 December 2010; these were 7.67 and 86 µmol kg^{-1} (31 % saturation), respectively. The maximum pH value observed was 8.38 at 7 m water depth on 15 October 2011 whereas the maximum DO value observed was 415 µmol kg^{-1} (165 % saturation) at 7 m water depth on 7 May 2011. These findings indicate that low DO and pH are persistently linked in the LJKF benthic environment.

4 Discussion

4.1 Temporal scales of dissolved oxygen and pH variability

Large ranges in DO and pH were observed on semidiurnal, diurnal and event time scales in the LJKF. This is not unexpected given that short-term fluctuations in many nearshore environments have been previously documented for many variables including temperature, nutrients, and DO (Kaplan et al., 2003; McPhee-Shaw et al., 2007; Moore et al., 2009; Jiang et al., 2011). These dynamics are likely to be representative of all nearshore environments that are under strong influences of wind, tide, and upwelling such as the major eastern boundary current systems (Benguela, California, Canary, Humboldt Current systems). We expected to observe a prominent diel signal from production and respiration of the kelp forest ecosystem as has been observed in

BGD
9, 4099–4132, 2012

other kelp forests (Delille et al., 2009), but diel modulations of DO and pH were not the dominant forcing observed in the LJKF. This could be due to strong cross-shore advection that may dampen the productivity signal or been counteracted by strong modulations from temperature. Diurnal changes in cross-shore advection can easily dominate in this study area due to intermittently enhanced diurnal winds associated with diurnal land-sea breeze (Pidgeon and Winant, 2005), wind- and tide-driven diurnal waves (Lerczak et al., 2001; Nam and Send, 2011), and sea/land breeze-driven resonant oscillations (Nam and Send, 2012).

The observed strong modulations of diurnal DO and pH fluctuations under equatorward currents (Fig. 4) are consistent with previous studies on the concentration and trapping of near-inertial (close to diurnal frequency in study location) internal wave energy under upwelling rather than downwelling conditions (Federiuk and Allen, 1996; Chant, 2001; Lerczak et al., 2001). Such internal waves are a primary mechanism that supplies nitrate to kelp forests (McPhee-Shaw et al., 2007), and are important for sustaining kelp growth. During this study, kelp forest ecosystem production in response to high-density, high-nutrient seawater led to elevated DO and pH on event time scales encompassing a few days to weeks; mean increases in DO and pH were related to alongshore current direction and velocity (Fig. 4, Table 1). Poleward flow following upwelling advects low DO (and low pH) water along the shelf and results in event-scale DO and pH changes that can be as significant as the effects of isopycnal shoaling on DO and pH (Send and Nam, 2012). Our observations here provide additional evidence for the significant role of alongshore current in event-scale DO and pH variability. In particular, biological production is expected to regulate mean DO and pH conditions for weeks at a time. High-density waters were present while alongshore current direction was equatorward. The transition from strong equatorward to poleward currents corresponded with the accumulation of DO, and uptake of CO_2 yielding increases in pH. Ecosystem production in response to the intrusion of high-density waters to shallow depths was evident in the DO and pH records at multiple times throughout the year (Table 1).

BGD
9, 4099–4132, 2012

4.2 Spatial scales of dissolved oxygen and pH variability

The largest gradients in DO and pH in this study occurred with changes in water depth. pH values not expected until 2100 at the surface in open ocean settings were observed frequently at 17 m depth in the LJKF (Caldeira and Wickett, 2003). The structure of the DO and pH gradient with depth was linked to the density structure of the water column and so future changes in stratification will alter the duration and frequency over which benthic communities are exposed to low DO and pH conditions.

Cross-shore gradients in DO and pH were greater than alongshore gradients. These results correspond to previously documented long alongshore correlation scales in currents (Winant, 1983; Lentz and Winant, 1986), water properties and nutrients (McPhee-Shaw et al., 2007). This suggests that fewer time series stations are needed in an alongshore direction relative to the cross-shore direction to accurately describe DO and pH dynamics.

DO and pH conditions at a given density decreased with decreasing distance from the shore. Mechanisms driving the cross-shore discrepancy among density, DO and pH warrant further investigation. The relationship between DO and pH was maintained at various distances from shore, but the DO and pH with density relationship had a decreasing offset towards the shore. Anomalies in the DO and density relationships have been previously observed on the San Diego margin. DO and pH isopleths shoaled towards the coast at a greater rate than isopycnals. The mechanisms that explained the DO anomaly at the Del Mar buoy included decreased subsurface primary production and strengthened poleward flows by the California Undercurrent (Nam et al., 2011), yet the extent to which these processes account for the nearshore anomalies in density with DO or pH observed during this study in the LJKF is unknown. The greatest cross-shore gradients in DO and pH were observed during the 2011 experiment. This experiment occurred further inshore (15 and 20 m bottom depth) than the 2010 cross-shore experiment (20 and 30 m bottom depth. At shallower bottom depths, benthic

BGD
9, 4099–4132, 2012

respiration may play a greater role in shoaling isopleths because benthic respiration processes are integrated over a smaller volume of water.

4.3 Relationship between dissolved oxygen and pH

The linear relationship between DO and pH was stable and coherent with depth, alongshore, and cross-shore direction in the context of this study (Fig. 6). The relationship is stronger with depth, and differences in the DO and pH relationship (e.g. slope) were observed between years. At high DO and high pH values there was nonlinearity. This nonlinearity may be explained by the expected changes in DO and pH with biological production and respiration (P:R) (Fig. 6c), which are nonlinear. At high values of DO and pH, production generates a greater increase in DO than pH. The P:R model was produced with mean temperature (14 °C), A_T (2252 µmol kg^{-1}), and salinity (33.4) conditions. It assumes an O_2:CO_2 Redfield ratio of −150 : 106 and an A_T:CO_2 ratio of −18 : 106. The overlap of the P:R model with the DO and pH relationship indicates that the biochemical consumption and production of O_2 is primarily responsible for the corresponding changes in DO and pH observed in the LJKF, and that calcification and dissolution of calcium carbonate play a more minor role.

There was no significant linear relationship between temperature and DO or pH at shallow depths contrasting to the firm relationship at deeper depths in the region (e.g., Fig. 6e,f and Fig. S1 in Nam et al., 2011). DO and pH are more affected by biochemical processes at shallow versus deep depths, and may account for the large deviations in the relationships between temperature and DO or pH.

4.4 Biological implications of dissolved oxygen and pH trends

pH and DO in the LJKF vary on multiple timescales with large ranges; biological responses to pH and DO also unfold over a range of timescales (Fig. 9). These processes involve biological organization from the genomic and molecular level to the whole organism. It is unknown whether and to what extent organisms actively or passively buffer themselves during rapid excursions of DO and pH. In the LJKF these rates of change can be as great as 62 µmol O_2 kg^{-1} h^{-1} and 0.16 pH units h^{-1}, respectively. However, a large range of environmental variability does not necessarily translate to extreme resistance to future OA and deoxygenation (Hofmann et al., 2011b). Decreasing DO and pH conditions could reach species-specific thresholds if organisms are operating at the limit of their physiological tolerances. The low values of DO and pH observed at 7 m in the LJKF are likely not biologically significant under present conditions. However the lower values of DO (< 90 µmol kg^{-1}) observed at 17 m are considered to be sublethal thresholds for coastal species of fishes, crustaceans and bivalves (Vaquer-Sunyer and Duarte, 2008). These groups are common and diverse within the kelp forest at depths deeper than 17 m where even lower DO concentrations occur (Parnell et al., 2006).

Future changes in water-column stability, the P:R ratio, upwelling dynamics (e.g. timing and intensity), wind patterns, and the sources and chemical properties of water that is advected horizontally and vertically into upwelling margins have the potential to alter the magnitude, frequency and duration of low DO and pH events experienced by the benthos. DO could reach hypoxic values at increasingly shallower depths and result in habitat compression (or expansion) for intolerant (or tolerant) species. We suggest that in eastern boundary current systems that biological sensitivity to changes in DO and pH will largely derive from changes in these dynamics that shoal low DO and pH waters from depth into nearshore benthic habitats (Feely et al., 2008; Hofmann et al., 2011a; Gruber, 2011), yet future changes in upwelling dynamics in the SCB remain critical questions for further research.

Laboratory studies have revealed that some resident species, and particularly their early life stages, are sensitive to the pH values observed in and around the LJKF during this study at 17 m. For example, larvae of the mussel *Mytilus californianus* a foundation species common in our study region, precipitated weaker, thinner and smaller shells and had lower tissue mass at pH_{tot} values of 7.83 and 7.63 versus 7.95 (Gaylord et al., 2011; pH values converted from NBS to total scale at 15 °C). pH was observed below 7.83 in the LJKF in deeper waters 32 % of the time. Thus, it is possible that *M.*

BGD
9, 4099–4132, 2012

californianus larvae are exposed to pH conditions in the present day that may elicit laboratory-observed biological responses to low pH. Additionally, the echinoplutei of another kelp forest species, the urchin *Lytechinus pictus*, were smaller and had altered gene expression in pH_{tot} treatments of 7.75 and 7.66 versus control conditions of 7.81 (O'Donnell et al., 2010; pH values converted from NBS to total scale at 18.5 °C). pH conditions less than 7.75 were observed 10 % of the time in the LJKF at 17 m water depth. These examples highlight the potential importance of vertical positioning for invertebrate larvae developing within the kelp forest. Full understanding of implications will require integration of DO and pH dynamics with research on how oxygen and pH influence energetics, calcification, sinking and swimming behavior.

5 Conclusions

In this study, we show that DO and pH in an eastern Pacific kelp forest were highly variable, tightly correlated, and reflected influences from many different processes including alongshore-current direction, internal tidal dynamics, and biological production. All of these features invoked large ranges in DO and pH. The most extreme and consistent temporal scales of variation in DO and pH were semidiurnal and diurnal. The high productivity of the kelp forest can increase DO and pH on event time scales in response to nutrient-replete water intrusion. This phenomenon may serve to alleviate biological stress following low DO and pH events. Thus, kelp forests and similar macrophyte regions might provide temporary refugia from acidification and deoxygenation when high levels of productivity elevate DO and pH values relative to surrounding waters. The spatial distribution of DO and pH in the LJKF was largely uniform in an alongshore direction, there were minor differences in the cross-shore direction, and there were drastic depth effects that are largely related to stratification of the water column. Future changes in warming and upwelling in the SCB will have implications for the exposure, duration, and frequency of low DO and pH experienced by benthic species and their early life stages. It is likely that nearshore communities along eastern boundary current

BGD
9, 4099–4132, 2012

systems are preadapted to the range of pH and DO observed during this study. However, communities may respond to rapid transitions at sharply defined critical thresholds rather than experience an extended transition to decreased pH. There is a need for more continuous monitoring of DO and pH along with relevant corresponding physical and biochemical variables, particularly where hypoxia lies near the shelf (Hofmann et al., 2011a). Such data will facilitate a mechanistic understanding of DO and pH trends in highly variable and potentially vulnerable coastal ecosystems.

Acknowledgement. We would like to acknowledge B. Peterson and Y. Takeshita who provided assistance with SeapHOx development and maintenance. We thank Andrew Dickson for providing access to his laboratory facilities to run DIC and TA samples. The ADCP data collected from the DM Buoy were provided by Uwe Send and SIO Ocean Time Series Group (http://mooring.ucsd.edu). We thank all those who assisted with field and diving support especially P. Zerofski, M. Navarro and G. Cook. We thank D. Holway, J. Leichter, and A. Dickson for comments on earlier drafts of this manuscript. This research was supported by NSF-OCE Award Nos. 0927445 and 1041062. This publication was developed under a Science to Achieve Results (STAR) Fellowship Assistance Agreement No. FP916973 awarded by the US Environmental Protection Agency (EPA). It has not been formally reviewed by the EPA. The views expressed in this publication are solely those of the authors.

References

Bograd, S. J., Castro, C. G., Di Lorenzo, E., Palacios, D. M., Bailey, H., Gilly, W., and Chavez, F. P.: Oxygen declines and the shoaling of the hypoxic boundary in the California Current, Geophys. Res. Lett., 35, L12607, doi:10.1029/2008GL034185, 2008.

Bray, N. A., Keyes, A., and Morawitz, W. M. L.: The California Current system in the Southern California Bight and the Santa Barbara Channel, J. Geophys. Res., 104, 7695–7714, 1999.

Caldeira, K. and Wickett, M. E.: Anthropogenic carbon and ocean pH, Nature, 425, 365, 2003.

Chant, R. J.: Evolution of near-inertial waves during an upwelling event on the New Jersey inner shelf, J. Phys. Oceanogr., 31, 746–764, 2001.

BGD
9, 4099–4132, 2012

Delille, B., Borges, A. V., and Delille, D.: Influence of giant kelp beds (*Macrocystis pyrifera*) on diel cycles of pCO_2 and DIC in the Sub-Antarctic coastal area, Estuar. Coast. Shelf S., 81, 114–122, 2009.

Dickson, A. G., Sabine, C. L., and Christian, J. R.: Guide to Best Practices for Ocean CO_2 Measurements, Vol. 3, 374 PICES Spec. Publ., Sidney, British Columbia, 2007.

Doney, S. C., Fabry, V. J., Feely, R. A., and Kleypas, J. A.: Ocean acidification: the other CO_2 problem, Annu. Rev. Mar. Sci., 1, 169–92, doi:10.1146/annurev.marine.010908.163834, 2009.

Doney, S. C., Ruckelshaus, M., Duffy, J. E., Barry, J. P., Chan, F., English, C. A., Galindo, H. M., Grebmeier, J. M., Hollowed, A. B., Knowlton, N., Polovina, J., Rabalais, N. N., Sydeman, W. J., and Talley, L. D.: Climate change impacts on marine ecosystems, Annu. Rev. Mar. Sci., 4, 11–37, doi:10.1146/annurev-marine-041911-111611, 2012.

Dong, C., Idica, E. Y., and McWilliams, J. C.: Circulation and multiple-scale variability in the Southern California Bight, Prog. Oceanogr., 82, 168–190, 2009.

Federiuk, J. and Allen, J. S.: Model studies of near-inertial waves in flow over the Oregon continental shelf, J. Phys. Oceanogr., 26, 2053–2075, 1996.

Feely, R. A., Sabine, C. L., Hernandez-Ayon, J. M., Ianson, D., and Hales, B.: Evidence for upwelling of corrosive “acidified” water onto the continental shelf, Science, 320, 1490, doi:10.1126/science.1155676, 2008.

Gaylord, B., Hill, T. M., Sanford, E., Lenz, E. A., Jacobs, L. A., Sato, K. N., Russel A. D., and Hettinger, A.: Functional impacts of ocean acidification in an ecologically critical foundation species, J. Exp. Biol., 214, 2586–2594, 2011.

Graham, M. H., Vásquez, J. A., and Buschmann, A. H.: Global ecology of the giant kelp *Macrocystis*: From ecotypes to ecosystems, Oceanogr. Mar. Biol., 45, 39–88, 2007.

Gruber, N.: Warming up, turning sour, losing breath: ocean biogeochemistry under global change, Phil. Trans. R. Soc. A, 369, 1980–1996, doi:10.1098/rsta.2011.0003, 2011.

van Heuven, S., Pierrot, D., Rae, J. W. B., Lewis, E., and Wallace, D. W. R.: MATLAB program developed for CO_2 system calculations. ORNL/CDIAC-105b. Carbon Dioxide Information Analysis Center, Oak Ridge National Laboratory, U. S. Department of Energy, Oak Ridge, Tennessee, doi:10.3334/CDIAC/otg.CO2SYS_MATLAB_v1.1, 2011.

Hofmann, A. F., Peltzer, E. T., Walz, P. M., and Brewer, P. G.: Hypoxia by degrees: Establishing definitions for a changing ocean, Deep-Sea Res. Pt. I, 58, 1212–1226, doi:10.1016/j.dsr.2011.09.004, 2011a.

BGD
9, 4099–4132, 2012

Variability of dissolved oxygen and pH

C. A. Frieder et al.

Hofmann, G. E., Smith, J. E., Johnson, K. S., Send, U., Levin, L. A., Micheli, F., Paytan, A., Price, N. N., Peterson B., Takeshita, Y., Matson, P. G., Crook, E. D., Kroeker, K. J., Gambi, M. C., Rivest, E. B., Frieder, C. A., Yu, P. C., and Martz, T. R.: High-frequency dynamics of ocean pH: A multi-ecosystem comparison, PLoSONE, 6, e28983, doi:10.1371/journal.pone.0028983, 2011b.

Jiang, Z.-P., Huang, J.-C., Dai, M., Kai, S. J., Hydes, D. J., Chou, W.-C., and Jan, S.: Short-term dynamics of oxygen and carbon in productive nearshore shallow water systems off Taiwan: Observations and modeling, Limnol. Oceanogr., 56(5), 1832–1849, 2011.

Kaplan, D. M., Largier, J. L., Navarrete, S., Guiñez, R., and Castilla, J. C.: Large diurnal temperature fluctuations in the nearshore water column, Estuar. Coast. Shelf S., 57, 385–398, 2003.

Keeling, R. F., Körtzinger, A., and Gruber, N.: Ocean deoxygenation in a warming world, Annu. Rev. Mar. Sci., 2, 199–229, doi:10.1146/annurev.marine.010908.163855, 2010.

Lentz, S. J. and Winant, C. J.: Subinertial currents on the Southern California shelf, J. Phys. Oceanogr., 16, 1737–1749, 1986.

Lerczak, J. A., Hendershott, M. C., and Winant, C. D.: Observations and modeling of coastal internal waves driven by a diurnal sea breeze, J. Geophys. Res., 106, 19715–19729, 2001.

Lluch-Cota, D. B., Wooster, W. S., and Hare, S. R.: Sea surface temperature variability in coastal areas of the northern Pacific related to the El Niño-Southern Oscillation and Pacific Decadal Oscillation, Geophys. Res. Lett., 28, 2029–2032, doi:10.1029/2000GL012429, 2001.

McClatchie, S., Goericke, R., Cosgrove, R., Auad, G., and Vetter, R.: Oxygen in the Southern California Bight: multidecadal trends and implications for demersal fisheries. Geohpys. Res. Lett., 37, L19602, doi:10.1029/2010GL044497, 2010.

McPhee-Shaw, E. E., Siegel, D. A., Washburn, L., Brzezinski, M. A., Jones, J. L., Leydecker, A., and Melack, J.: Mechanisms for nutrient delivery to the inner shelf: Observations from the Santa Barbara Channel, Limnol. Oceanogr., 52, 1748–1766, 2007.

Martz, T. R., Connery, J. G., and Johnson, K. S.: Testing the Honeywell Durafet® for seawater pH applications, Limnol. Oceanogr. Methods, 8, 172–184, 2010.

Moore, T. S., Nuzzio, D. B., Di Toro, D. M., and Luther III, G. W.: Oxygen dynamics in a well mixed estuary, the lower Deleware Bay, USA, Mar. Chem., 117, 11–20, 2009.

Nam, S. and Send, U.: Direct evidence of deep-water intrusions onto the continental shelf via surging internal tides, J. Geophys. Res., 116, C05004, doi:10.1029/2010JC006692, 2011.

Nam, S. and Send, U.: Resonant diurnal oscillations and mean alongshore flows driven by sea/land breeze forcing in the coastal Southern California Bight, J. Phys. Oceanogr., in review, 2012.

Nam, S., Kim, H-J., and Send, U.: Amplification of hypoxic and acidic events by La Niña conditions on the continental shelf off California, Geophys. Res. Lett., 38, L22602, doi:10.1029/2011GL049549, 2011.

North, W. J., James, D. E., and Jones, L. G.: History of kelp beds (*Macrocystis*) in Orange and San Diego Counties, California, Hydrobiologia, 260/261, 277–283, 1993.

O'Donnell, M. J., Todgham, A. E., Sewell, M. A., Hammond, L. M., Ruggiero, K., Fangue, N. A., Zippay, M. L., and Hofmann, G. E.: Ocean acidification alters skeletogenesis and gene expression in larval sea urchins, Mar. Ecol. Prog. Ser., 398, 157–171, 2010.

Parnell, P. E., Dayton, P. K., Lennert-Cody, C., Rasmussen, L. L., and Leichter, J. J.: Marine reserve design: Optimal size, habitats, species affinities, diversity, and ocean microclimate, Ecol. Appl., 16, 945–962, 2006.

Parnell, P. E., Miller, E. F., Lennert-Cody, C. E., Dayton, P. K., Carter, M. L., and Stebbins, T. D.: The response of giant kelp (*Macrocystis pyrifera*) in southern California to low-frequency climate forcing, Limnol. Oceanogr., 55, 2686–2702, 2010.

Pidgeon, E. J. and Winant, C. D.: Diurnal variability in currents and temperature on the continental shelf between Central and Southern California, J. Geophys. Res., 110, C03024, doi:10.1029/2004JC002321, 2005.

Pineda, J.: Circulation and larval distribution in internal tidal bore warm fronts, Limnol. Oceanogr., 44, 1400–1414, 1999.

Pringle, J. M. and Riser, K.: Remotely forced nearshore upwelling in Southern California, J. Geophys. Res., 108, 3131, doi:10.1029/2002JC001447, 2003.

Send, U. and Nam, S.: Relaxation from upwelling: the effect on dissolved oxygen on the continental shelf, J. Geophys. Res., doi:10.1029/2011JC007517, in press, 2012.

Vaquer-Sunyer, R. and Duarte, C. M.: Thresholds of hypoxia for marine biodiversity, P. Natl. Acad. Sci. USA, 105, 15452–15457, doi:10.1073/pnas.0803833105, 2008.

Winant, C. D.: Longshore coherence of currents on the Southern California Shelf during the summer, J. Phys. Oceanogr., 13, 55–64, 1983.

Table 1. Event-scale mean increases in dissolved oxygen (ΔDO) and pH (ΔpH) proceeding intrusion of high-density water ($\sigma > 25.1\,\mathrm{kg\,m^{-3}}$) at 7 m water depth. v and u indicate the mean velocity ($\mathrm{cm\,s^{-1}}$) of alongshore and cross-shore currents, respectively, between 5 and 30 m for 7 d before and after the event. Negative values are equatorward or offshore for v and u, respectively. Positive values of ΔDO and ΔpH indicate mean increases from before to after the event. Events are ordered by magnitude of ΔDO.

Event start	Mooring	v before	v after	u before	u after	ΔDO	ΔpH
14 Jul 2010	B	−1.6	4.3	0.5	1.0	66	0.07
26 Apr 2011	A	−3.8	10.9	0.7	2.5	63	0.10
26 Apr 2011	D	−3.8	10.9	0.7	2.5	62	0.10
27 Nov 2010	A	−4.4	5.9	1.2	0.8	35	0.03
31 Jul 2011	A	0.8	0.0	1.2	3.4	35	0.01
21 Aug 2010	A	0.3	4.2	−0.7	0.1	25	0.03
21 Aug 2010	B	0.3	4.2	−0.7	0.1	−2	−0.02

BGD
9, 4099–4132, 2012

Table 2. Low dissolved oxygen (ΔDO) and pH (ΔpH) events at 7 m water depth at mooring A. Event start date is day that low-pass filtered DO and pH fell below 200 µmol kg^{-1} and 7.9 units, respectively, and duration is the and duration is the time spent below these values. ND = no data.

Event start	Duration	Mean DO	Mean pH	Mean density
04 Sep 2010	1.8	136	7.82	25.5
12 Sep 2010	> 1.4	167	7.88	25.0
03 Sep 2011	4.5	180	nd	25.0
21 Sep 2011	2.3	189	nd	25.0
01 Oct 2011	1.1	184	nd	25.0
16 Oct 2011	3.1	184	nd	25.0

BGD
9, 4099–4132, 2012

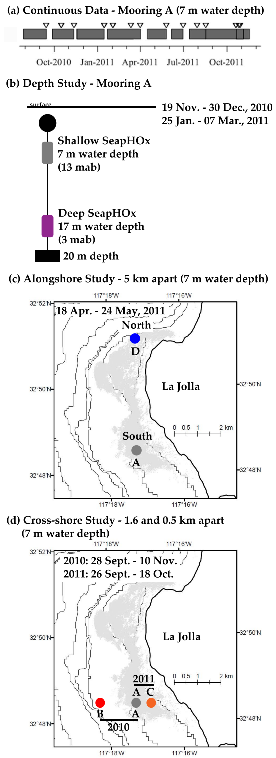

Fig. 1. Placement of SeapHOx sensors among moorings to characterize DO and pH differences **(a)** over time, **(b)** with depth, **(c)** in an alongshore direction, and **(d)** in a cross-shore direction. Bathymetric contours are in 10 m increments (10–60 m depth). At least one discrete sample (upside-down triangles) was taken per SeapHOx deployment to calibrate the pH sensor. Color scheme of moorings corresponds with subsequent figures. Grey shading in **(c)** and **(d)** depicts maximum extent of the La Jolla Kelp Forest based on aerial surveys from 1989–2009 (California Department of Fish and Game).

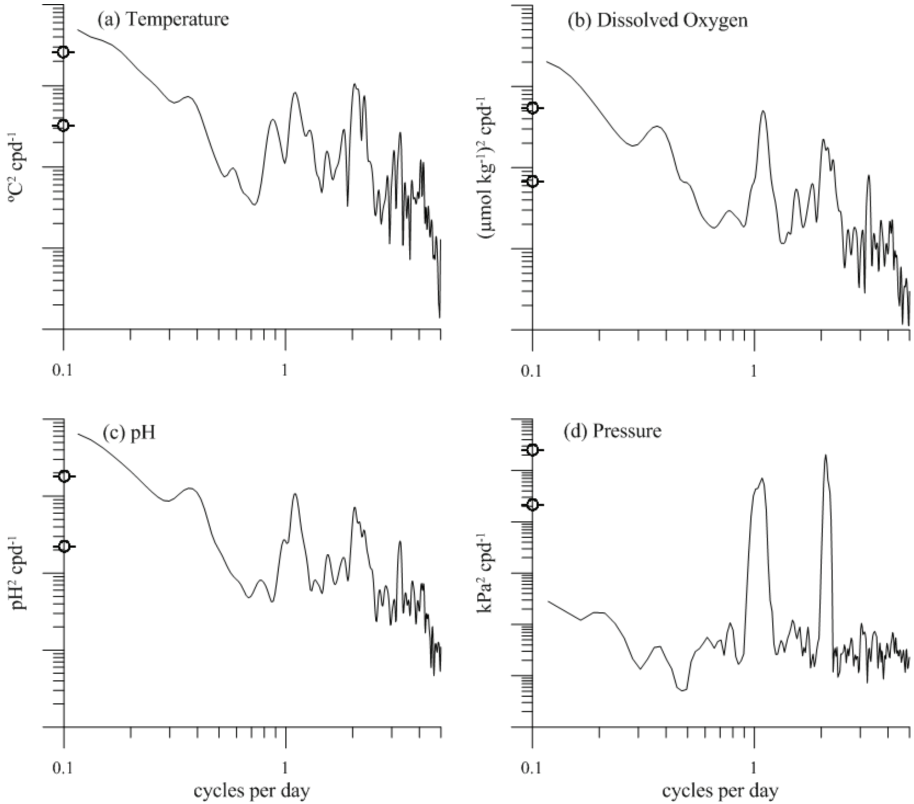

Fig. 2. Frequency power spectra (cycles per day) from mooring A at 7 m water depth 29 July–13 September 2010 for **(a)** temperature, **(b)** dissolved oxygen, **(c)** pH and **(d)** pressure. The circles on the left side of each graph denote the critical scale for 95 % confidence in energy peaks.

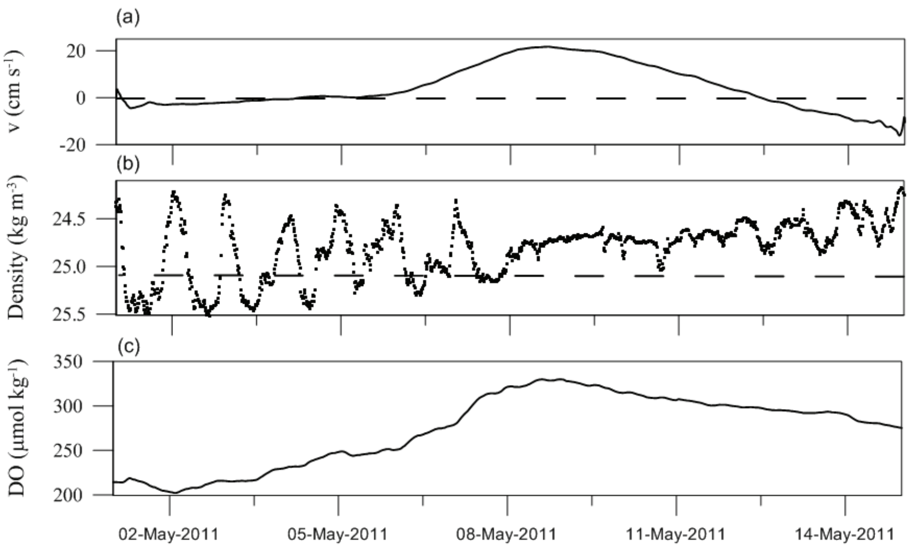

Fig. 3. Event-scale increases in dissolved oxygen (DO) following the intrusion of high-density seawater ($\sigma > 25.1\,kg\,m^{-3}$) at 7 m below the surface at mooring D. **(a)** Mean alongshore current velocity between 5 and 30 m at the Del Mar Buoy, **(b)** time series of density and **(c)** time series of 2-d smoothed DO from 26 April 2011–16 May 2011. Density scale is reversed. Positive alongshore velocities indicate poleward flow.

BGD
9, 4099–4132, 2012

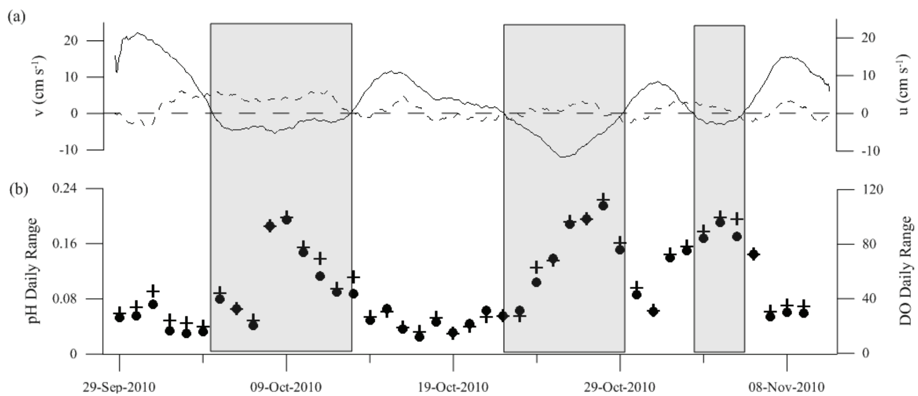

Fig. 4. (a) Mean alongshore current velocity (v: solid) and mean cross-shore current velocity (u: dotted) between 5 and 30 m from the Del Mar Buoy and **(b)** daily range in pH (circles) and dissolved oxygen (DO: crosses) from mooring A at 7 m water depth. Grey-shaded rectangles indicate time periods when alongshore velocities are equatorward (negative). See Fig. 8 for corresponding time-series of density, DO and pH.

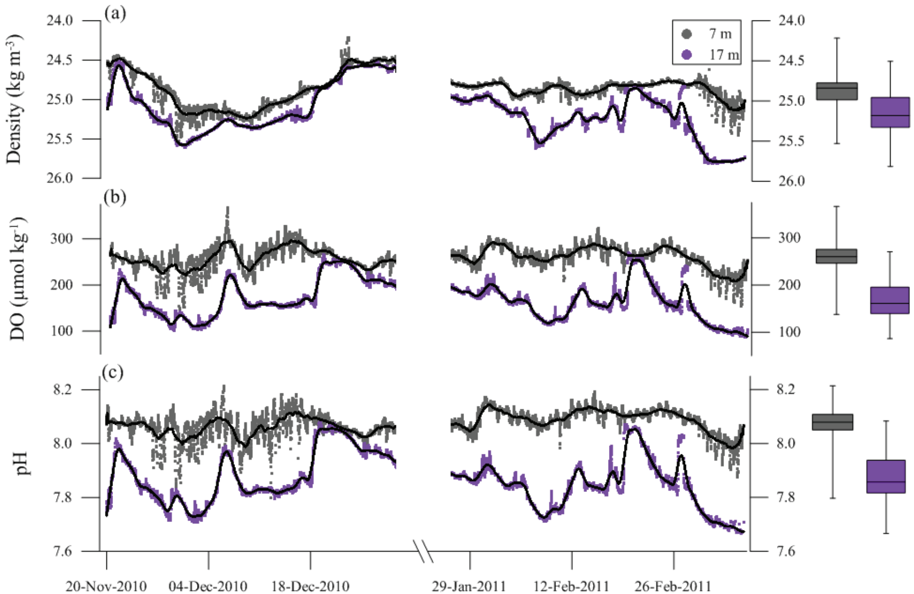

Fig. 5. Density, dissolved oxygen (DO) and pH comparisons between 7 m (grey) and 17 m (purple) at mooring A during two separate deployments. Time series and corresponding box plots of **(a)** density, **(b)** dissolved oxygen and **(c)** pH. Black solid lines are 2-d smoothed data. Density scale is reversed. Box plots at right depict the minimum, maximum, median, lower quartile and upper quartile for corresponding time-series data.

BGD
9, 4099–4132, 2012

Variability of dissolved oxygen and pH

C. A. Frieder et al.

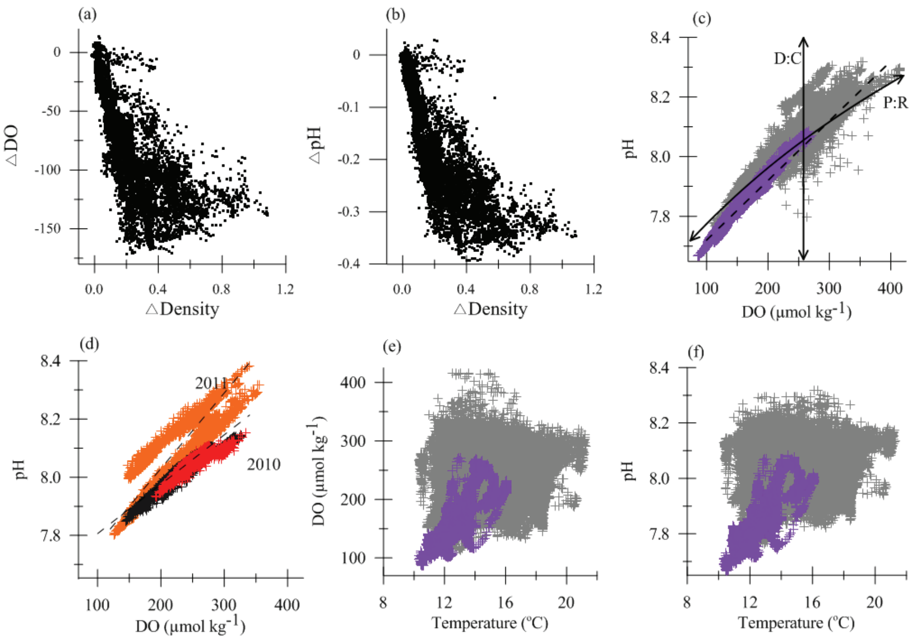

Fig. 6. Scatterplots of **(a)** density difference (ΔDensity) and dissolved oxygen difference (ΔDO) between 7 and 17 m at mooring A, and **(b)** ΔDensity and pH difference (ΔpH) between 7 and 17 m at mooring A. Includes all data from Fig. 5. **(c)** Scatter plot of DO and pH at 7 m (grey hatches) and 17 m (purple hatches) below the surface from all SeapHOx deployments from 10 July 2010–19 October 2011. Dashed black line is the linear relationship between pH and DO for all data regardless of depth. Solid black lines represent expected changes in DO and pH with production and respiration (P:R) and dissolution and calcification of $CaCO_3$ (D:C). **(d)** Scatterplot of DO and pH with varying distance from shore. Data and marker colors correspond with Fig. 8. Dashed black lines are the linear relationship between DO and pH in 2010 and 2011. Scatterplots of **(e)** temperature and DO and **(f)** temperature and pH for all data as in **(c)**.

BGD
9, 4099–4132, 2012

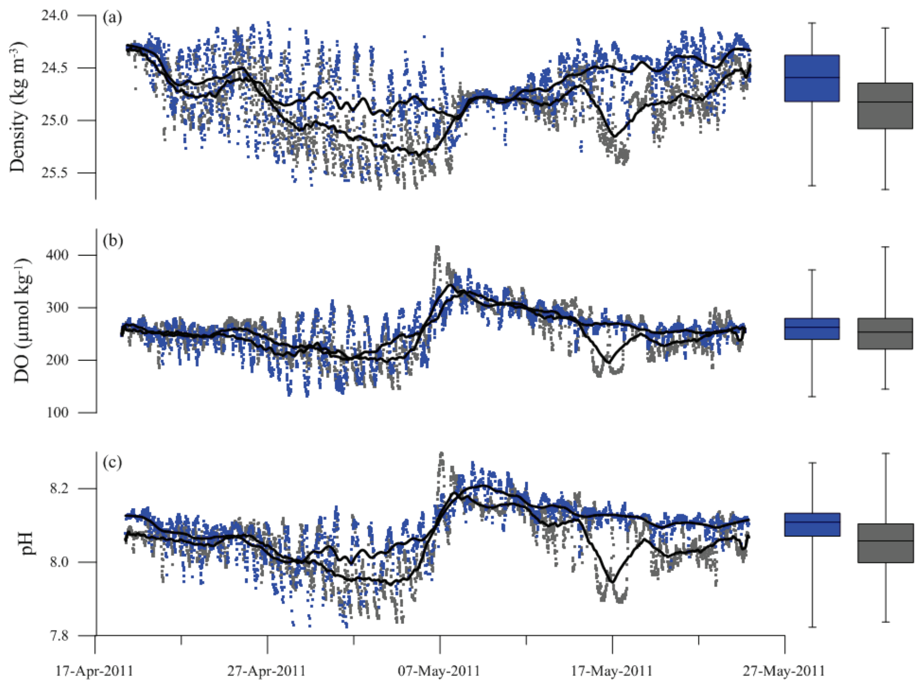

Fig. 7. Alongshore comparisons in density, dissolved oxygen (DO) and pH in the south and north La Jolla Kelp Forest. Time series and corresponding box plots of **(a)** density, **(b)** DO and **(c)** pH at south LJKF (mooring A; grey) and north LJKF (mooring D; blue) at 7 m below the surface. Black solid lines are 2-d smoothed data. Density scale is reversed. Box plot depicts the minimum, maximum, median, lower quartile and upper quartile for corresponding time-series data.

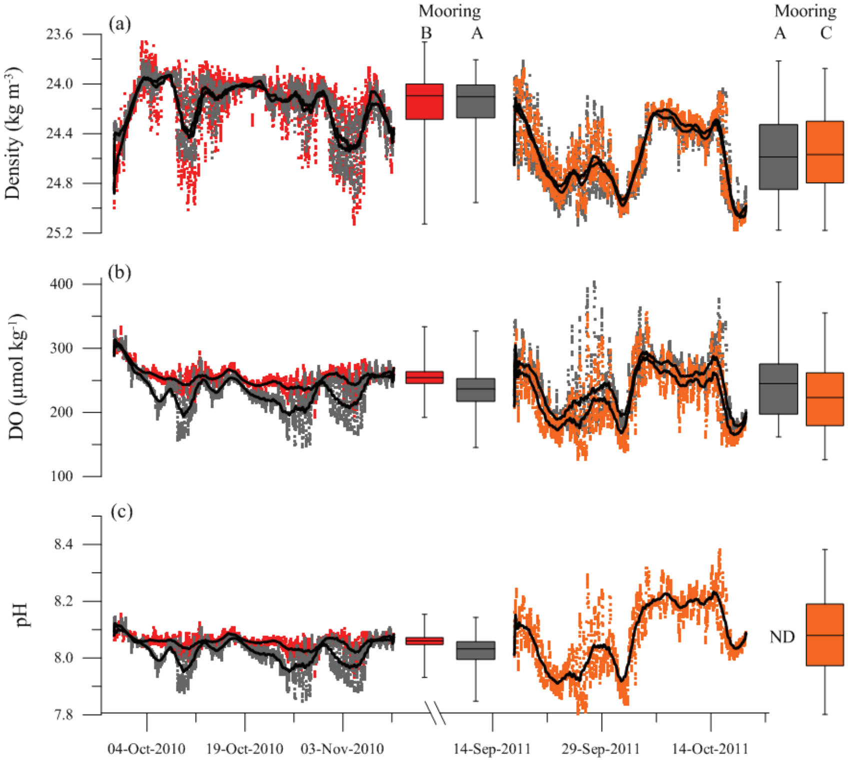

Fig. 8. Cross-shore differences in time-series and corresponding box plots of **(a)** density, **(b)** dissolved oxygen (DO) and **(c)** pH. From 28 September 2010–10 November 2010 one SeapHOx was deployed at mooring B, 3.5 km from the coast (red) and the other SeapHOx was deployed at mooring A, 1.9 km from the coast (grey). From 26 September 2011–18 October 2011 one SeapHOx was deployed at mooring A, 1.9 km from the coast (grey) and the other SeapHOx was deployed at mooring C, 1.4 km from the coast (orange). Black solid lines are 2-d smoothed data. Density scale is reversed. Box plot depicts the minimum, maximum, median, lower quartile and upper quartile for corresponding time-series data. ND = no data.

BGD
9, 4099–4132, 2012

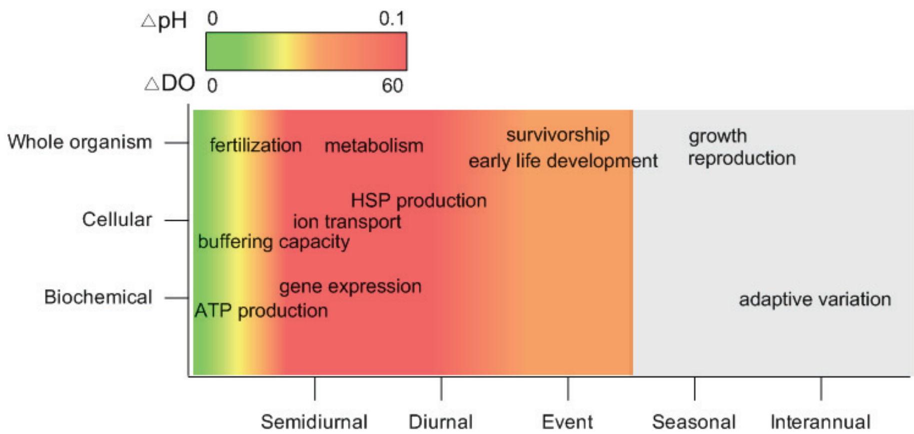

Fig. 9. Synoptic view of mean range in pH and DO (ΔpH and ΔDO) at 7 m depth in the La Jolla kelp forest over varying timescales and levels of biological organization. Superimposed on ΔpH and ΔDO are biological processes which may be sensitive to changes in DO and pH and the timescales over which they occur. Grey shaded area indicates uncharacterized time scales.

BGD
9, 4099–4132, 2012